JETIR.ORG ISSN: 2349-5162 | ESTD Year : 2014 | Monthly Issue
JOURNAL OF EMERGING TECHNOLOGIES AND INNOVATIVE RESEARCH (JETIR)
An International Scholarly Open Access, Peer-reviewed, Refereed Journal

NUMERICAL STUDY OF HYDROMAGNETIC CONVECTIVE HEAT AND MASS TRANSFER FLOW EG-BASED MoS_2-SiO_2 NANO FLUIDS IN CHEMICAL PARAMETERS IN CIRCULAR ANNULAR REGION

Dr. J. SIVA SHANKARA RAO
Lecturer in Mathematics, Government College (A), Ananthapuramu-515001, A.P., India,

Abstract

An attempt has been made to investigate combined effect of variable viscosity andthermo diffusion on hydromagnetic convective heat transfer flow of Eg-based MoS_2 and SiO_2Nanofluids in cylindrical annulus. The nonlinear coupled equations governing the flow heat and mass transfer have been executed by emplying Galarkin finite element method with quadratic intrepolitation function. It is found that the important parametric of increase in Viscosity parameter (B) decays velocity, enhances temperature and concentration in the flow region.

Keywords **:** Variable viscosity, Thermal radiation, Eg-based MoS_2 and SiO_2Nanofluids, Cylindrical annulus.

1. INTRODUCTION

Materials like ethylene glycol, oils and water etc., having low conductivity are less impressive in heat conducting phenomenon.Thermal conductivity and heat transfer coefficient of base materials can be boosted through inclusion of nanoparticles (Choi and Eastman [7]; Buongiorno [6]. The alignment of solid particles encompassing 1-100 nm size in base materials is known as nanofluids.Investigating approach to enhance heat transportation in engineering utilization for illustration electronic mechanisms chilling equipped with nanofluids, energy stowing structures, heat exchangers, food processing and lubrication equipment employing nanofluids has been examined by numerous scholars. Hossain [13] examined the effect of Joule heating and viscous dissipation in flow of viscous fluid. Eastman et al[10] disclosed the measurement of thermal conductivity of $C_2H_6O_2$ (ethylene glycol) fluid with Cu-nanofluids. Sheikholeslami and Ganji [33] studied the behaviour of shape factor on forced convective flow of nanofluid with Lorentz forces. Some researchers examined nanofluids under numerous features in the refs. (Hayat et al[12];Yin et al [39]; Zhang et al [42]).

In general, in most recent research areas, heat transfer enhancement in forced convection is desirable ([Behzadmehr et al[4], Bianco et al [5] and Santra [30]), but there is still a debate on the effect of nano-particles on heat transfer enhancement in natural convection applications. Abu-Nada [1] investigated the effect of variable viscosity and thermal conductivity of Al_2O_3-water nanofluid on heat transfer enhancement in natural convection. Das et al [9] have studied mixed convective magneto hydrodynamic flow in a vertical channel filled with nanofluids. Sree Devi et al. [34] has investigated mixed convective heat and mass transfer flow of nanofluids in concentric annulus with constant heat flux. Sudarsana Reddy and Chamka, [35] have analyzed the Soret and Dufour effects on MHD convective flow of Al_2O_3-water and TiO2-water nanofluids past a stretching sheet in porous media with heat generation/absorption. Madhusudhana Reddy et al., [17] have presented Numerical study of Convective Flow of CuO-water and Al_2O_3-water Nanofluids in cylindrical annulus. Sulochana et al [36] have discussed heat and mass transfer flow in cylindrical annulus in presence of heat sources.

Thermal motion of the charged particles produces electromagnetic radiation called thermal radiation. Every matter emits thermal radiation at a temperature greater than absolute zero (absolute temperature is also called thermodynamic temperature). Heat transfer in the presence of thermal radiation has many applications in

physics, industrial engineering, space technology for example gas cooled nuclear reactors, aerodynamics rockets, large open water reservoirs, thermal power engineering and so forth. Rosseland approximation has been considered by numerous researchers for radiation effect. This type of approximation comprises dimensionless variables called radiation parameter and Prandtl number which are supportable for linearized Rosseland approximation if the temperature difference between the plate and ambient liquid is small. Radiative flow over a stretched surface is examined by Cortell [8]. Sheikholeslami et al. [33] investigated MHD two phase nano-liquid flows with thermal radiation. Reddy et al. [28] examined the impact of nonlinear radiation in three-dimensional MHD flow of ferromagnetic liquid subject to temperature dependent viscosity. Natural convection along a vertical isothermal plate with linear and nonlinear thermal radiations is studied by Pantokratoras [25]. Consequences of nonlinear thermal radiation and heterogeneous-homogeneous reactions in flow based on $Ag–H_2O$ and $Cu–H_2O$ nano-material by a stretched cylinder is presented by Qayyum et al. [27]. Vijayalakshmi [38] has considered the hydromagnetic convective heat transfer flow of Swcnt-water nanofluid in a circular annuls.

An inorganic Molybdenum disulfide (MoS_2) material is designated as a metal dichalcogenide. It's composed of alternating layers of molybdenum and sulphur atoms. It appears as the crystal molybdenite, which is a black-silver solid. It is commonly utilized as a stabilizing agent due to its low interfacial characteristics and durability. MoS_2 has a low reactivity and is undisturbed by weak acids and oxidant. Thus, every molybdenum atom is sandwiched with both trigonal sulphur prisms in a hexagonal close-packed configuration. The sulphur sheets are loosely held together by van der Waals force. Molybdenum disulphide nanomaterials are typically composed of nano-sized MoS_2 dispersed in water-based liquids. Zhang et al. [41] have experimentally organized Newtonian molybdenum disulphide nanofluids that are homogeneous and steady. Identical to graphene, molybdenum disulphide does have a wide bandgap configuration comprising single and multilayer sheets. Using Laplace transform technique, Arif et al. [2] examined Maxwell fluid flow containing uniformly distributed molybdenum disulfide and graphene nanoparticles with engine oil as base fluid. They found that the rate of heat transfer of molybdenum disulfide nanoparticles is greater than graphene nanoparticles. Liu et al. [16] conducted experiments on the coefficient of thermal volumetric expansion, heat conductivity, and heat capacity. Khan et al. [14] examined various shape factor effects on the Molybdenum disulphide hydromagnetic nanoparticles flow and water as a conveying fluid in a vertical porous medium.Masood Khan et al [19] have described the irreversibility process analysis for SiO_2-MoS_2/water-based flow over a rotating and stretching cylinder. Swirling flow of fluid containing, (SiO_2) and (MoS_2) nanoparticles analyze via Cattaneo-Christov theory analyzed by Zhang et al [40].Umair Khan et al[37] and Maraj et al[18] discriminated the mixed Convective Magneto Flow of $SiO_2–MoS_2/C_2H_6O_2$ Hybrid Nanoliquids Through a Vertical Stretching/Shrinking Wedge: Stability Analysisinside an isothermal semi vertical inverted cone with porous boundary. Shamshuddin et al [32] have compared and discussed to thermal exploration of convective transportation of ethylene glycol based magnetized nanofluid flow in porous cylindrical annulus utilizing MoS_2 and Fe_3O_4 nanoparticles with inconstant viscosity. Recently Mumtaz Khan and Amer Rasheed [21] have briefly discussed the Slip velocity and temperature jump effects on molybdenum disulfide MoS_2 and silicon oxide SiO_2 hybrid nanofluid near irregular 3D surface.

In the majority of silicon dioxides, the silicon atom shows tetrahedral coordination, with four oxygen atoms surrounding a central Si atom (see 3-D Unit Cell). Thus, SiO_2 forms 3-dimensional network solids in which each silicon atom is covalently bonded in a tetrahedral manner to 4 oxygen atoms. In contrast, CO_2 is a linear molecule. The starkly different structures of the dioxides of carbon and silicon are a manifestation of the double bond rule. Based on the crystal structural differences, silicon dioxide can be divided into two categories: crystalline and non-crystalline (amorphous). In crystalline form, this substance can be found naturallyoccurring as quartz, tridymite (high-temperatureform), cristobalite (high-temperature form), stishovite (high-pressure form), and coesite (high-pressure form). On the other hand, amorphous silica can be found in nature as opal and diatomaceous earth. Quartz glass is the form of intermediate state between this structure. All of this distinct crystalline forms always have the same local structure around Si and O. In α-quartz the Si–O bond length is 161 pm, whereas in α-tridymite it is in the range 154–171 pm. The Si–O–Si angle also varies between a low value of 140° in α-tridymite, up to 180° in β-tridymite. In α-quartz, the Si–O–Si angle is 144°. Muhammad Nabil Fikri Mohamad et al[20] have discussed the Heat Transfer Performance Of TiO_2 –SiO_2Nanofluid in Water-Ethylene Glycol Mixture. Azmi et al[3] were described the Heat transfer and friction factor of water based TiO_2 and SiO_2nanofluids under turbulent flow in a tube. Noor Sabeeh Majeed et al [23] have been study the Effect of SiO_2Nanofluids on Heat Transfer in Double Pipe Heat Exchanger. Namburu*et al.* [22] were used another types of nanoparticles SiO_2 with different particle sizes (20, 50, 100) nm

to calculate the viscosity and specific heat of nanofluid with ratio 60:40 water and ethylene glycol base fluid; giving a new correlation employing experimental data.

The objective of this study is to investigate and highlight the effect of variable viscosity andthermal radiation on convective heat transfer flow of MoS_2 and SiO_2 nanofluids in the case of cylindrical annulus. The behaviour of velocity, temperature and concentration is analyzed at different axial positions. The shear stress and the rate of heat and mass transfer have also been obtained for variations in the governing parameters.

2. FORMULATION OF THE PROBLEM

We analyse the mixed convective flow of SiO_2 nanofluid and MoS_2nanofluid in a vertical circular annulus through a porous medium whose walls are maintained at a constant heat and concentration. The flow, temperature and concentration in the fluid are assumed to be fully developed. Both the fluid and porous region have constant physical properties and the flow is a mixed convection flow taking place under thermal and molecular buoyancies and uniform axial pressure gradient. The Boussinesq approximation is invoked so that the density variation is confined to the thermal and molecular buoyancy forces.The momentum, energy and diffusion equations are coupled and non-linear. Also the flow is unidirectional along the axial direction of the cylindrical annulus. Making use of the above assumptions the governing equations are

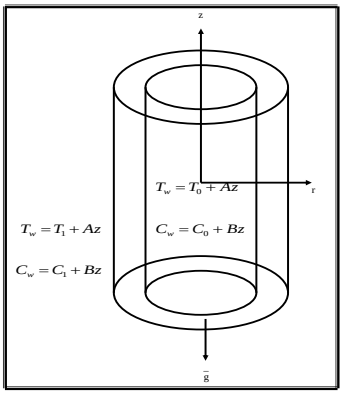

Fig.1 : CONFIGURATION OF THE PROBLEM

$$-\frac{\partial p}{\partial z}+\frac{1}{\rho_{nf} r}\frac{\partial}{\partial r}\left((\mu_{nf}(T)\,\mathrm{r}\frac{\partial u}{\partial r})\right)-(\frac{\mu_{nf}}{\rho_{nf} k})u-\frac{\sigma_f \mu_e^2 H_0^2}{\rho_{nf} r^2}+(\rho\beta)_{nf}(T-T_o)=0 \quad (2.1)$$

$$(\rho C_p)_{nf}\, u\frac{\partial T}{\partial z}=k_{nf}(\frac{\partial^2 T}{\partial r^2}+\frac{1}{r}\frac{\partial T}{\partial r})-\frac{1}{r}\frac{\partial (rq_r)}{\partial r}+\mu_{nf}(\frac{du}{dr})^2+(\sigma_{nf}\mu_e^2 H_o^2)(u^2) \quad (2.2)$$

$$u\frac{\partial C}{\partial z}=D_B\left(\frac{\partial^2 C}{\partial r^2}+\frac{1}{r}\frac{\partial C}{\partial r}\right)-k_c^{'}C+\frac{D_m K_T}{T_s}\left(\frac{\partial^2 T}{\partial r^2}+\frac{1}{r}\frac{\partial T}{\partial r}\right)- \quad (2.3)$$

where u is the axial velocity in the porous region, T , C are the temperature and concentration of the fluid, k is the permeability of porous medium, k_f is the thermal diffusivity, F is a function that depends on Reynolds number, the microstructure of the porous medium and D_B is the molecular diffusivity, D_m is the mass diffusivity, K_T mass diffusion ratio, β is the coefficient of the thermal expansion, q_R is the radiation absorption coefficient, Cp is the specific heat, ρ is density,g is gravity, ρ_{nf} is the effective density. μ_{nf} is the effective dynamic viscosity, k_{nf} is the thermal conductivity of the nanofluid.

The relevant boundary conditions are

$$u=0,\quad T=T_i,\qquad C=C_i \qquad on\ \ r=a,$$
$$u=0,\quad T=T_o,\qquad C=C_o \qquad on\ \ r=a+s \quad (2.4)$$

We now define the following non-dimensional variables for the fully developed laminar flow in the presences of radial magnetic field, the velocity depend only on the radial coordinate and all the other physical variables except temperature, concentration and pressure are functions of r and z, z being the vertical co-ordinate .

We now define the following non-dimensional variables

$$\eta^*=\frac{r}{a},z^*=\frac{z}{a},\mathrm{s}^*=\frac{s}{a},p^*=\frac{pa^2}{\rho\nu_f^2},\pi=\frac{dp^*}{dz},u^*=(\frac{\nu_f}{a})\mathrm{u},\theta=\frac{T-T_o}{T_i-T_o},C^*=\frac{C-C_o}{C_i-C_{o\,i}} \quad (2.5)$$

The effective density of the nanofluid is given by

$$\rho_{nf}=(1-\varphi)\rho_f+\varphi\rho_s \quad (2.6)$$

Where ϕ is the solid volume fraction of nanoparticles. Thermal diffusivity of the nanofluid is

$$\alpha_{nf}=\frac{k_{nf}}{(\rho C_p)_{nf}} \quad (2.7)$$

Where the heat capacitance C_p of the nanofluid is obtained as

$$(\rho C_p)_{nf}=(1-\varphi)(\rho C_p)_f+\varphi(\rho C_p)_s \quad (2.8)$$

And the thermal conductivity of the nanofluid k_{nf} for spherical nanoparticles can be written as

$$\frac{k_{nf}}{k_f} = \frac{(k_s + 2k_f) - 2\phi(k_f - k_s)}{(k_s + 2k_f) + \phi(k_f - k_s)} \quad (2.9)$$

The thermal expansion coefficient of nanofluid can determine by

$$(\rho\beta)_{nf} = (1-\varphi)(\rho\beta)_f + \varphi(\rho\beta)_s \quad (2.10)$$

Also the effective dynamic viscosity of the nanofluid given by

$$\mu_{nf} = \frac{\mu_f}{(1-\varphi)^{2.5}}, \quad \sigma_{nf} = \sigma_f\left(1 + \frac{3(\sigma-1)\phi}{\sigma+2-(\sigma-1)\phi}\right), \sigma = \frac{\sigma_s}{\sigma_f} \quad (2.11)$$

where the subscripts nf, f and s represent the thermo physical properties of the nanofluid, base fluid and the nanosolid particles respectively and ϕ is the solid volume fraction of the nanoparticles. The thermo physical properties of the nanofluid are given in Table 1.

The thermo physical properties of the nanofluids are given in Table 1 (See ***Oztop and Abu-Nada*** **[24]**).

Table – 1

Physical properties	Fluid phase (Ethylene Glycol)	**MoS_2**	**SiO_2**
C_p(j/kg K)	**2430**	**397.21**	**703**
ρ(kg m^3)	**1115**	**5060**	**2200**
k(W/m K)	**0.253**	**904.4**	**1.2**
βx10^{-5} 1/k)	**99**	**2.8424**	**0.056**
σ	**0.05**	**10^6**	**10^7**

Introducing these non-dimensional variables, the governing equations in the non-dimensional form are (on removing the stars)

$$\left(\frac{\partial^2 u}{\partial \eta^2} + \frac{1}{\eta}\frac{\partial u}{\partial \eta} - \mathrm{B}\left(\frac{\partial u}{\partial \eta}\right)\left(\frac{\partial T}{\partial \eta}\right)\right) = A_1 A_3 \pi\, \mathrm{e}^{B\theta} + A_1\left(D^{-1} + \frac{A_6 M^2\, \mathrm{e}^{B\theta}}{\eta^2}\right)u - A_1 A_4 G\, \mathrm{e}^{B\theta}(\theta) \quad (2.12)$$

$$A_2\left(1 + \frac{4Rd}{3}\right)\left(\frac{\partial^2 \theta}{\partial \eta^2} + \frac{1}{\eta}\frac{\partial \theta}{\partial \eta}\right) + \mathrm{EcPr}(\mathrm{e}^{-B\theta})\left(\frac{du}{d\eta}\right)^2 + M^2 Ec\,\mathrm{Pr}(u^2) = A_5\,\mathrm{Pr}\,u \quad (2.13)$$

$$\left(\frac{\partial^2 C}{\partial \eta^2} + \frac{1}{\eta}\frac{\partial C}{\partial \eta}\right) - \gamma C = Sc\,u + ScSr\left(\frac{\partial^2 \theta}{\partial \eta^2} + \frac{1}{\eta}\frac{\partial \theta}{\partial \eta}\right) - \gamma C \quad (2.14)$$

where

$B = m(T_0 - T_i)$ (Viscosity parameter), $G = \frac{g\beta(T_e - T_i)a^3}{\nu^2}$ (Grashof number), $M^2 = \frac{\sigma\mu_e^2 H_0^2}{a\nu}$ (magnetic parameter), $D^{-1} = \frac{a^2}{k}$ (Inverse Darcy parameter), $P_r = \frac{\mu C_p}{k_f}$ (Prandtl number), $Rd = \frac{4\sigma^{\bullet} T_o^3}{k_f \beta_R}$ (Thermal radiation parameter), $Ec = \frac{\nu_f}{a^2 C_p(T_i - T_0)}$ (Eckert number), $Sc = \frac{\nu}{D_B}$ (Schmidt number), $\gamma = \frac{k_c a^2}{D_B}$ (Chemical Reaction parameter), $So = \frac{D_m K_T(T_0 - T_{i)}}{T_s(C_0 - C_i)}$ (Soret parameter)

$$A_1 = \frac{1}{(1-\varphi)^{2.5}}, A_2 = (1-\varphi) + \varphi\left(\frac{\rho_s}{\rho_f}\right)\ A_1 = \frac{1}{(1-\varphi)^{2.5}}, \ A_2 = (1-\varphi) + \varphi\left(\frac{\rho_s}{\rho_f}\right), \ A_3 = 1 - \varphi + \varphi\frac{(\rho C_p)_s}{(\rho C_p)_f},$$

$$A_4 = 1 - \varphi + \varphi\left(\frac{(\rho\beta)_s}{(\rho\beta)_f}\right), \quad A_5 = \frac{k_{nf}}{k_f} \quad A_6 = \left(1 + \frac{3(\sigma-1)}{\sigma+2-(\sigma-1)\phi}\right), \sigma_{nf} = \sigma_f A_6, \ \sigma = \frac{\sigma_s}{\sigma_f}$$

The corresponding non-dimensional conditions are

$$u = 0, \quad \theta = 1, \ C = 1 \quad on \quad \eta = 1$$
$$u = 0, \quad \theta = 0, \ \mathrm{C} = 0 \quad on \quad \eta = 1 + s \quad (2.15)$$

3. FINITE ELEMENT ANALYSIS

The finite element analysis with quadratic polynomial approximation functions is carried out along the radial distance across the circular duct. The behavior of the velocity, temperature and concentration profiles has been discussed computationally for different variations in governing parameters. The Galerkin method has been

adopted in the variational formulation in each element to obtain the global coupled matrices for the velocity, temperature and concentration in course of the finite element analysis.

Choose an arbitrary element e_k and let u^k, θ^k and C^k be the values of u, θ and C in the element e_k. We define the error residuals as

$$E_p^k = \frac{d}{d\eta}\left(\eta\frac{du^k}{d\eta}\right) - B\left(\frac{du^k}{d\eta}\right)\left(\frac{d\theta^k}{d\eta}\right) + A_1A_4\eta G\,e^{B\theta^k}(\theta^k) - A_1\left(D^{-1} + \frac{A_6M^2e^{B\theta^k}}{\eta^2}\right)\eta u^k - \quad (3.1)$$

$$-A_1A_3\,e^{B\theta^k}$$

$$E^k{}_\theta = \frac{A_2}{\Pr}\left(1+\frac{4Rd}{3}\right)\frac{d}{d\eta}\left(\eta\frac{d\theta^k}{d\eta}\right) - A_5\eta u^k \quad (3.2)$$

$$E^k{}_c = \frac{d}{d\eta}\left(\eta\frac{dC^k}{d\eta}\right) - \eta Scu^k - \gamma C^k + ScS_r\frac{d}{d\eta}\left(\eta\frac{d\theta^k}{d\eta}\right) - \gamma C^k \quad (3.3)$$

where u^k, θ^k & C^k are values of u, θ& C in the arbitrary element e_k. These are expressed as linear combinations in terms of respective local nodal values.

$$u^k = u_1^k\psi_1^k + u_2^k\psi_1^k + u_3^k\psi_3^k,\quad \theta^k = \theta_1^k\psi_1^k + \theta_2^k\psi_2^k + \theta_3^k\psi_3^k,\quad C^k = C_1^k\psi_1^k + C_2^k\psi_2^k + C_3^k\psi_3^k$$

where ψ_1^k, ψ_2^k --------- etc are Lagrange's quadratic polynomials.

Galarkin's method is used to convert the partial differential Equations (3.1) – (3.3) into matrix form of equations which results into 3x3 local stiffness matrices. All these local matrices are assembled in a global matrix by substituting the global nodal values and using inter element continuity and equilibrium conditions. The resulting global matrices have solved by iterative procedure until the convergence i.e $|u_{i+1}-u_i|<10^{-6}$ is obtained.

4. SKIN FRICTION,NUSSELT NUMBER AND SHERWOOD NUMBER

The Skin friction (τ) is evaluated using the formula $\tau = \left(\frac{du}{d\eta}\right)_{\eta=1,1+s}$.

The rate of heat transfer (Nusselt number) is evaluated using the formula $Nu = -\left(\frac{d\theta}{d\eta}\right)_{\eta=1,1+s}$.

The rate of mass transfer (Sherwood number) is evaluated using the formula $Sh = -\left(\frac{dC}{d\eta}\right)_{\eta=1,1+s}$

5. COMPARISON

Table 1 : Numerical comparison of Nusselt number(Nu) results for different Prandtl numbers

Pr	Shaiq et al [31]	Salawu et al.[29]	Khan et al.[15]	**Present values**
0.07	0.0656	0.0656	0.0673	**0.065023**
0.20	0.1691	0.1691	0.1678	**0.168243**
0.70	0.4539	0.4539	0.4549	**0.454089**
2.00	0.9114	0.9114	0.9109	**0.910234**
7.00	1.8854	1.8854	1.8894	**1.874570**
20.00	3.3539	3.3539	3.3537	**3.345475**

6. RESULTS AND DISCUSSION

From the fig(2a-2c) we observe that velocity increases while temperature and nanoconcentration decrease in Ethylene Glycol(Eg) based MoS_2 and SiO_2 nanofluids in the entire flow region as Grashof number (G) uprises. This is due to the fact that increase in G enhances the thickness of momentum boundary layer and decays thermal and solutal boundary layersthickness in both types of nanofluids.

Higher the Lorentz force (M) smaller the velocity(u), nanoconcentartion(C), larger the temperature(θ) in both types of nanofluids. (Fig.3a-3c). This amounts to the fact that increase in M gives rise to retarding force which reduces the velocity in boundary layers. The thickness of momentum and solutal boundary layers decays while the thermal boundary layer becomesthicker with the higher values of M in both types of nanofluids.

Lesser the porous parameter (K) smaller the velocity in both types of naonofluids (fig.4a). θ and C enhance in Eg based MoS_2 nanofluid while they depreciate in Eg based SiO_2nanofluid (fig.4b & 4c). This may be attributed to the fact that momentum boundary layer becomes thinner with the decreasing values of porous

permeability in both types of naonofluids, thickness of thermal and solutal boundary layers enhances in Eg based MoS_2 nanofluid while in Eg based SiO_2nanofluid it decreases.

Higher the thermal radiation (Rd) smaller the *u*, larger θ and C in Eg based MoS_2 nanofluid while in Eg based SiO_2*u*, θ enhance, C reduces with rising values of Rd. (Fig 5a-5c). This can be attributed to the fact that an increase in Rd decays the thickness of momentum boundary layer while grows the thickness of solutal and thermal boundary layers.

Higher the dissipative energy (Ec) smaller *u* in both types of nanofluids. θ&C are enhanced in Eg based MoS_2 nanofluid while in Eg based SiO_2 nanofluid, they reduce in the flow region. (Figs.6a-6c). The velocity(*u*) descends throughout the momentum boundary layer in both types of nanofluids with the increasing values of Ec. Thermal and solutal boundary layers become thicker in Eg based MoS_2 nanofluid while in Eg based SiO_2 nanofluid they become thinner.

Increase in viscosity parameter (B)leads to a decay in velocity(*u*) in both types of nanofluids (figs.7a). θ& C are enhanced in Eg based MoS_2 nanofluid while in Eg based SiO_2 nanofluid they experience reduction in the flow region. (Figs.7b & 7c). This is due to the fact that higher the values of B/E1/δ1 lesser the momentum boundary layer thickness in both types of nanofluids. Thermal and solutal boundary layers become thicker in Eg based MoS_2 nanofluid while in Eg based SiO_2 nanofluid they become thinner.

Figs.8a-8c demonstrate the effect of Prandtl number (Pr) on *u*, θ and C. Lesser the thermal diffusivity smaller *u*, larger θ in both types of nanofluids (figs. 8a & 8b). C enhances in Eg based MoS_2 nanofluid and reduces in Eg based SiO_2 nanofluid (fig. 8c). This can be attributed to the fact that lesser the thermal diffusivity smaller the momentum boundary layer and larger the thermal boundary layer in both types of nanofluids. Solutal boundary layer thickness increases in Eg based MoS_2 nanofluid and decreases in Eg based SiO_2 nanofluid with the increasing values of Prandtl number.

The values of *u*, θ and C in Eg based MoS_2 nanofluid are relatively greater than those in Eg based SiO_2 nanofluid with the increasing values of G/Ec/Pr. The values of C in Eg based MoS_2 nanofluid are relatively greater than those in Eg based SiO_2 nanofluid while the values of *u* and θ in Eg based SiO_2 nanofluid are higher than those in Eg based MoS_2 nanofluid with the increasing values of M/K/Rd/ B.

The skin friction (τ), rate of heat transfer (Nusselt number (Nu)) and rate of mass transfer (Sherwood number (Sh)) are presented (Tabs. 2 and 3). It is observed that skin friction (τ) increases with a rise inGrashofnumber (G) and reverse outcomes are noticed in case of viscosity parameter (B) in both types of nanofluidsat η = 1. It is noticed that an increment in magnetic parameter (M)/ porous parameter (K)/ thermal radiation (Rd)/ Eckert number (Ec) /Prandtl number (Pr) increases τ in Eg based MoS_2 nanofluid and decreases τ in Eg based SiO_2 nanofluid at η = 1. It is seen that skin friction (τ) decreases with a growth in G/ M/ K/ Rd/Pr in both types of nanofluids at η = 2 but opposite results are seen in case of Ec/ B.

It is observed that rate of heat transfer decreases in Eg based MoS_2 nanofluid and increases in Eg based SiO_2 nanofluid with the increasing values of G/M/K/Rd/Ec/B/Pr at inner cylinder. Nusselt number (Nu) enhances with the viscosity parameter (B) in both types of nanofluids at outer cylinder. Rate of heat transfer augments in Eg based MoS_2 nanofluid and decays in Eg based SiO_2 nanofluid with an increment in G/M/K/Rd/Ec while reverse outcomes are noted in case of Pr at outer cylinder.

It is noticed that Sherwood number (Sh) increases in both types of nanofluids with a growth in Grashof number (G) while the rate of mass transfer (Sh) decays in Eg based MoS_2 nanofluid and enhances in Eg based SiO_2 nanofluid with the increasing values of M/K/Rd/Ec/ B/Pr at η = 1.It is observed that an increment in G/M/K/Rd/Ec/B/Pr increases Sherwood number (Sh) in Eg based MoS_2 nanofluid while decreases Sherwood number in Eg based SiO_2 nanofluid at η = 2.

The values of skin friction (τ) and Sherwood number (Sh) in Eg based MoS_2 nanofluid are relatively greater than those in Eg based SiO_2 nanofluid while the values of Nusselt number (Nu) in Eg based MoS_2 nanofluid are relatively lesser than those in Eg based SiO_2 nanofluid for the variations in G/M/K/Rd/Ec/ B/Pr at an inner cylinder. The values of skin friction (τ) and Nusselt number (Nu) in Eg based MoS_2 nanofluid are relatively higher than those in Eg based SiO_2 nanofluid while the values of Sherwood number in Eg based SiO_2 nanofluid are relatively larger than those in Eg based MoS_2 nanofluid for the variations of the same parameters G/ M/ K/ Rd/ Ec/ B/ Pr at the outer cylinder.

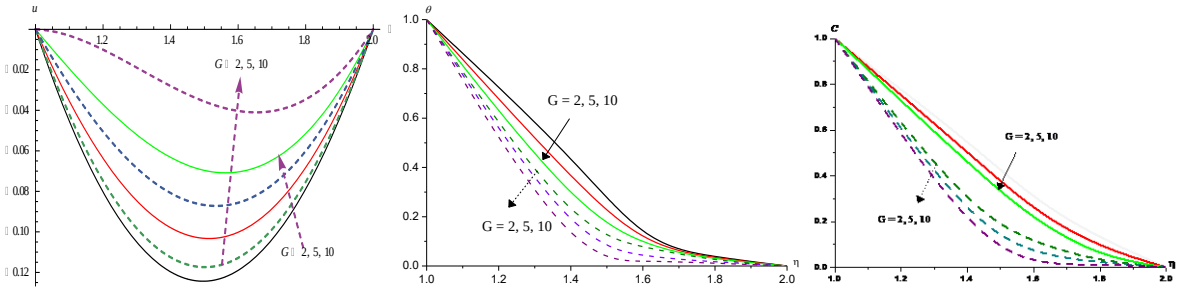

Fig.2 : Variation of [a] Velocity(u), [b] Temperature(θ), Nano-Concentration[C] with G
M=0.5, K=0.01, Rd=2.5, Ec=2.5, B=0.2, Pr=0.71

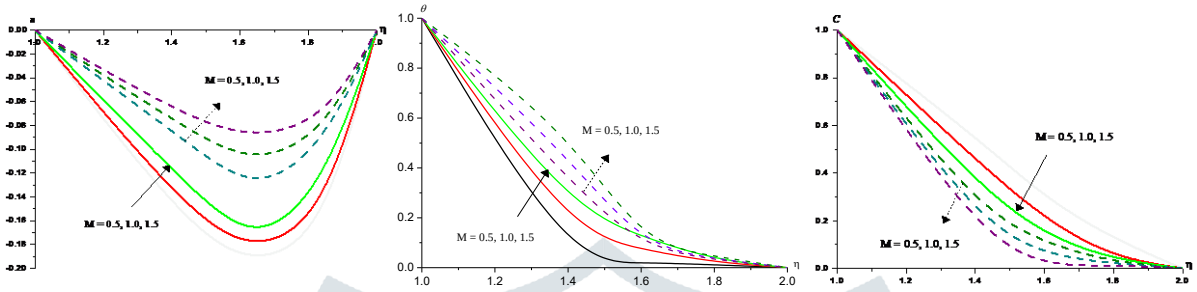

Fig.3 : Variation of [a] Velocity(u), [b] Temperature(θ), Nano-Concentration[C] with M
G=2, K=0.01, Rd=2.5, Ec=2.5, B=0.2, Pr=0.71

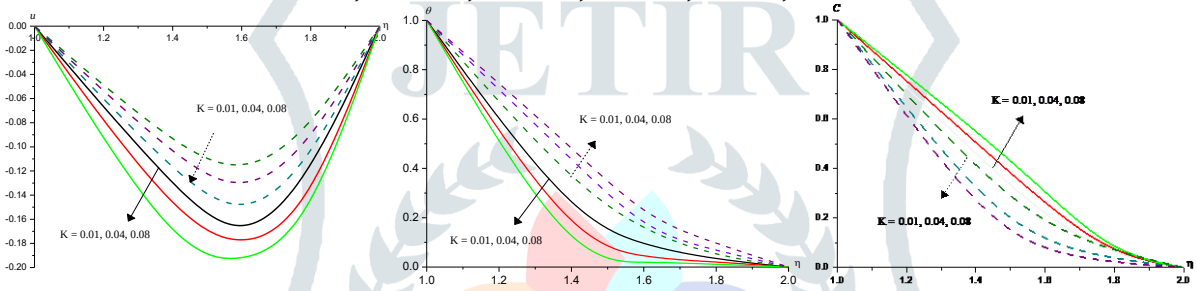

Fig.4 : Variation of [a] Velocity(u), [b] Temperature(θ), Nano-Concentration[C] with K
G=2, M=0.5, Rd=2.5, Ec=2.5, B=0.2, Pr=0.71

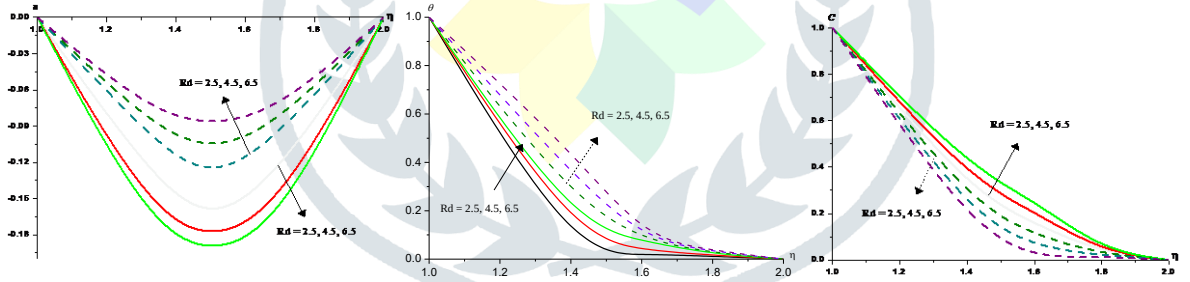

Fig.5 : Variation of [a] Velocity(u), [b] Temperature(θ), Nano-Concentration[C] with Rd
G=2, M=0.5, K=0.01, Ec=2.5, B=0.2, Pr=0.71

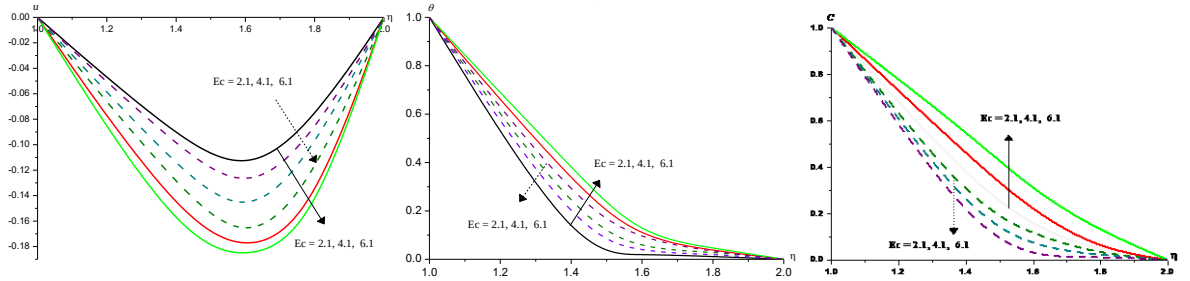

Fig.6 : Variation of [a] Velocity(u), [b] Temperature(θ), Nano-Concentration[C] with Ec
G=2, M=0.5, K=0.01, Rd=2.5, B=0.2, Pr=0.71

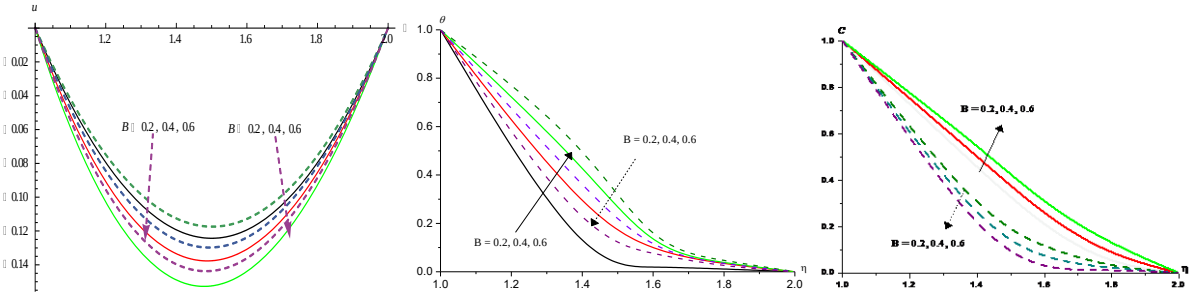

Fig.7 : Variation of [a] Velocity(u), [b] Temperature(θ), Nano-Concentration[C] with B
G=2, M=0.5, K=0.01, Rd=2.5, Ec=2.5, Pr=0.71

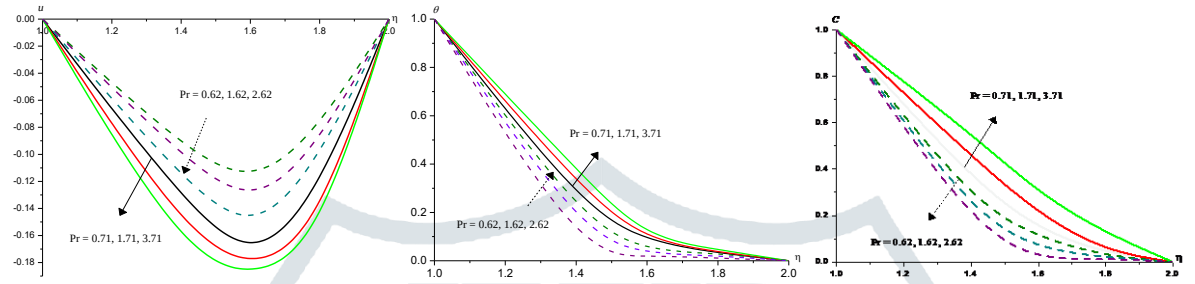

Fig.8 : Variation of [a] Velocity(u), [b] Temperature(θ), Nano-Concentration[C] with Pr
G=2, M=0.5, K=0.01, Rd=2.5, Ec=2.5, B=0.2

Table 2 : Skin friction (τ), Nusselt number(Nu) and Sherwood number(Sh) with MoS_2& SiO_2 – Ethylene Glycol (Eg) at η = 1

Parameter		MoS2 – Ethylene Glycol			SiO2 – Ethylene Glycol		
		τ(1)	Nu(1)	Sh(1)	τ(1)	Nu(1)	Sh(1)
G	2	-0.496599	1.0001	2.3933	-0.466525	0.99962	3.95412
	5	-0.391422	0.999999	2.38253	-0.293798	1.00216	5.40598
	10	-0.201074	1.0001	2.38512	-0.00600138	1.00343	6.54497
M	0.5	-0.496599	1.0001	2.3933	-0.466525	0.99962	3.95412
	1.0	-0.502152	0.999995	2.38106	-0.463261	0.999881	5.40544
	1.5	-0.496481	0.999994	2.38117	-0.457929	0.999444	6.5438
K	0.01	-0.496623	1.0001	2.3933	-0.466547	0.99962	3.95412
	0.04	-0.505636	0.999996	2.38098	-0.466538	1.00008	5.40534
	0.08	-0.50562	0.999995	2.38098	-0.466525	0.999986	6.54357
Rd	2.5	-0.496623	1.0001	2.3933	-0.46663	0.998671	3.95291
	4.5	-0.505652	0.999997	2.38098	-0.466577	1.00016	5.40498
	6.5	-0.505652	0.999998	2.38098	-0.466532	0.99999	6.54383
Ec	2.1	-0.496623	1.0001	2.3933	-0.466571	1.00262	3.95362
	4.1	-0.505652	0.999988	2.38098	-0.466575	1.00293	5.40478
	6.1	-0.505652	0.99998	2.38099	-0.466575	1.00269	6.54301
B	0.2	-0.496623	1.0001	2.3933	-0.466547	0.999635	3.95412
	0.4	-0.580189	0.999995	2.37997	-0.534495	0.999756	5.405
	0.6	-0.667539	0.999993	2.37883	-0.614054	0.9994	6.54302
Pr	0.71	-0.496623	1.00001	2.3933	-0.466592	1.00374	3.95322
	1.71	-0.505652	0.999996	2.38098	-0.466549	0.999786	5.40541
	3.71	-0.505652	0.999984	2.38099	-0.466451	0.990691	6.54588

Table 3 : Skin friction (τ), Nusselt number(Nu) and Sherwood number (Sh) with MoS_2& SiO_2 – Ethylene Glycol(Eg) at η = 2

Parameter		MoS2 – Ethylene Glycol			SiO2 – Ethylene Glycol		
		τ(2)	Nu(2)	τ(2)	Nu(2)	τ(2)	Nu(2)
G	2	0.497433	0.999995	0.439836	0.472184	0.99652	0.235403
	5	0.437923	0.999992	0.443829	0.393495	0.99444	0.119759
	10	0.351067	0.999989	0.442242	0.262445	0.99318	0.066827
M	0.5	0.497433	0.999995	0.439836	0.472184	0.99652	0.235403
	1.0	0.486862	0.999997	0.444731	0.469174	0.99643	0.120494
	1.5	0.481676	0.999999	0.444848	0.459251	0.99501	0.068587
K	0.1	0.497409	0.999993	0.439836	0.472159	0.99652	0.235403
	0.4	0.490032	0.999994	0.444782	0.472178	0.99623	0.120542
	0.8	0.490048	0.999995	0.444789	0.472192	0.99549	0.068683
Rd	0.5	0.497409	0.999993	0.439836	0.472254	0.98659	0.236066
	1.5	0.490016	0.999997	0.444782	0.472197	0.99350	0.120696
	5.0	0.490008	0.999998	0.444789	0.472141	0.99159	0.068591
Ec	0.2	0.497409	0.99999	0.439836	0.472185	0.99313	0.235553
	0.4	0.490016	1.00001	0.444781	0.472183	0.99302	0.120661
	0.6	0.490006	1.00003	0.444786	0.472178	0.99244	0.068766
B	0.2	0.497409	0.999993	0.439836	0.472159	0.99653	0.235403
	0.4	0.523934	0.999996	0.445402	0.504108	0.99685	0.120871
	0.6	0.561474	0.999998	0.446097	0.539428	0.99769	0.069283
Pr	0.71	0.497409	0.999981	0.439836	0.472198	0.99219	0.235686
	1.71	0.490016	0.999994	0.444782	0.472167	0.99661	0.120525
	3.71	0.490029	1.000014	0.444791	0.472075	1.00732	0.068319

7. CONCLUSIONS

The effect of variable viscosity on MHD convective heat transfer flow of Eg based MoS_2 and SiO_2nanofluids through a porous medium in a vertical channel have been analysed by executing the governing equations numerically.The findings of this analysis are:

- Increase in Gashof number (G) increases velocity and reduces temperature and nanoconcentration in Eg-MoS_2 and SiO_2nanofluids. Higher the Lorentz force/Lesser the porous permeability (K) smaller the velocity, nanoconcentration and larger the temperature .
- Increase in Rd/Ec, decays the velocity and grows the temperature and nanoconcentration in both types of nanofluids.
- Increase in Viscosity parameter(B),decays velocity,enhances temperature and concentration in the flow region.
- The skin friction(τ) decays with increase in G/ M/ K/ Rd/Pr and opposite effect is noticed in the case of Ec/ B at the outer cylinder(η=2) in both types of nanofluids.
- Rate of heat transfer enhances in Eg based MoS_2 nanofluid and decays in Eg-SiO_2nanofluid with increase in G/M/K/Rd/Ec.
- Increase in G/M/K/Rd/Ec/Pr increases Sh in Eg-MoS_2nanofluid and decreases in Eg-SiO_2nanofluiud at η=2.

8. REFERENCES

[1]. Abu-Nada, E: Effect of variable viscosity and thermal conductivity of Al_2O_3-water nanofluid on heat transfer enhancement in natural convection, Int J heat Fluid Flow, V.30, 679-690(2009).

[2]. Arif M.*et al.*, Enhanced heat transfer in working fluids using nanoparticles with ramped wall temperature: Applications in engine oil, Adv. Mech. Eng. (2019)

[3]. Azmi W.H., Sharma K.V., Sarma P.K., Mamat R., and Najafi G., Heat transfer and friction factor of water based TiO2 and SiO2 nanofluids under turbulent flow in a tube,International Communications in Heat and Mass Transfer 59 30-38 (2014).

[4]. Behzadmehr, A., Saffar-Avval, M., Galanis, N: Prediction of turbulent forced convection of a nanofluid in a tube with uniform heat flux using a two phase approach, Int J Heat Fluid Flow, V.28, 211-219(2007).

[5]. Bianco V., Chiacchio. F., Manca, O., Nardini, S: Numerical investigation of nanofluids forced convection in circular tubes, J. Appl Therm Eng, V.29, 3632-3642(2009).

[6]. Buongiorne,J:Convective transport in Nanofluids,Journal Heat transfer 128,pp.250-250(2006)

[7]. Choi S.U.S and Eastman,A:Enhancinh thermal conductivity of fluids with Nanoparticles,ASME publications-Fed231,pp.99-106(1995)

[8]. Cortell R. Fluid flow and radiative nonlinear heat transfer over a stretching sheet. J King Saud Univ Sci, 7,pp.26:161 (2014).

[9]. Das, S., Jana, R.N., and Makinde, O.D : Mixed convective magneto hydrodynamic flow in a vertical channel filled with nanofluids, Engineering science and technology an International Journal, V.18, 244-255(2015).

[10]. Eastman,J.A.,S.U.S Choi,S,Li,W.Yu, and J.Thomson:Anomalously increased effective thermal conductivities of Ethylene Glycol based Naqnofluids containing Copper nanoparticles,Applications Physical Letters,V.78,pp.718-720(2001)

[11]. Emad M Abo-Eldahab and Mohamed A El Aziz: Blowing/Suction effect on hydromagnetic heat transfer by mixed convection from an inclined continuous stretching surface with internal heat generation/absorption., Int. J.Termal Sciences,V.43(7),pp.709-719(2004).

[12]. Hayat,T,S,Ullah,M.I.Khan. and A.Aisaedi:On framing potential features of Swcnt's and MNcnt's in Mixed convective flow ,Result Physical,V,8,pp.357-364(2018c)

[13]. Hossain,A:Viscous and Joule heating effects on MHD free convection flow with variable plate temperature,International Journal Heat Mass trqansfer,35,pp.3485-3487(1992)

[14]. Khan I. , Shape effects of MoS_2 nanoparticles on MHD slip flow of molybdenum disulphide nanofluid in a porous medium, J. Mol. Liq. (2017)

[15]. Khan M.I., Khan S.A., Hayat T., Waqas M., Alsaedi A., Modeling and numerical simulation for flow of hybrid nanofluid (SiO2/ C3H8O2) and (MoS2/C3H8O2) with entropy optimization and variable viscosity, Int. J. Num. Meth. Heat & Fluid Flow. 22 (8) (2020) 3939–3995.

[16]. Liu J. *et al.* Measurement of the anisotropic thermal conductivity of molybdenum disulfide by the time-resolved magneto-optic Kerr effect, J. Appl. Phys.,(2014)

[17]. Madhusudhana Reddy, Y., Rama Krishna, G.N. and Prasada Rao, D.R.V: Numerical study of Convective Flow of CuO-water and Al_2O_3-water nanofluids in cylindrical annulus, Int. Journal of Research & Development in Tech., Vol. 7, Issue 3, 142-148 (2017).

[18]. Maraj, E.N., Iqbal, Z., Azhar, E., Mehmood, Z.: A comprehensive shape factor analysis using transportation of MoS_2-SiO_2/H_2O inside an isothermal semi vertical inverted cone with porous boundary. Res. Phys. **8**, 633–641 (2018)

[19]. Masood Khan, Mahnoor Sarfraz, Sabba Mehmood and Malik Zaka Ullah, Irreversibility process analysis for *SiO*2-*MoS*2/water-based flow over a rotating and stretching cylinder, Journal of Applied Biomaterials & Functional Materials (JABFM),1-15, (July 2022) DOI: 10.1177/22808000221120329
[20]. Muhammad Nabil Fikri Mohamad1, Wan Azmi Wan Hamzah, Khamisah Abdu Hamid, Rizalman Mamat :Heat Transfer Performance Of Tio2–SiO2 Nanofluid In Water-Ethylene Glycol Mixture**,** Journal of Mechanical Engineering, Vol SI 5(1), 39-48, 2018
[21]. Mumtaz Khan, Amer Rasheed : Slip velocity and temperature jump effects on molybdenum disulfide MoS2 and silicon oxide SiO2 hybrid nanofluid near irregular 3D surface, Alexandria Engineering Journal (2021) 60, 1689–1701, https://doi.org/10.1016/j.aej.2020.11.019
[22]. Namburu P.K., Kulkarni, D.P., Dandekar, A., Das, D.K., Experimental investigation of viscosity and specific heat of silicon dioxide nanofluids, Micro and Nano Letters, 2, no. 3, 2007, p. 67.
[23]. Noor Sabeeh Majeed, Shaymaa Mahdi Salih, Hussam Nadum Abda Lraheemal Ani, Basma Abbas Abdulmajeed, Paul Constantin Albu, Gheorghe Nechifor: Study the Effect of SiO2 Nanofluids on Heat Transfer in Double Pipe Heat Exchanger, Revista de Chimie**,** Rev. Chim., 71 (5), 2020, 117-124, https://doi.org/10.37358/RC.20.5.8119
[24]. Oztop H. F. and Abu-Nada E., "Numerical study of natural convection in partially heated rectangular enclosures filled with nanofluids," *International Journal of Heat and Fluid Flow*, vol. 29, no. 5, pp. 1326–1336, (2008).
[25]. Pantokratoras A. Natural convection along a vertical isothermal plate with linear and nonlinear Rosseland thermal radiation. Int J Therm Sci ;84:151–7 (2014).
[26]. Putra, N., Roetzel W, Das, S.K: Natural convection of nanofluids, Heat and Mass Transfer, V.39 (8-9), 775-784(2003).
[27]. Qayyum S, Khan MI, Hayat T, Alsaedi A. A framework for nonlinear thermal radiation and homogeneous-heterogeneous reactions flow based on silverwater and copper-water nanoparticles: A numerical model for probable error. Results Phys;7:1907–14 (2017).
[28]. Reddy JVR, Surunamma V, Sandeep N. Impact of nonlinear radiation on 3D magnetohydrodynamic flow of methanol and kerosene based ferrofluids with temperature dependent viscosity. J Mol Liquids; 236:39–100 (2017).
[29]. Salawu S.O., Obalalu A.M., Fatunmbi E.O., Oderinu R.A., Thermal Prandtl-Eyring hybridized MoS2-SiO2/C3H8O2 and SiO2-C3H8O2 nanofluids for effective solar energy absorber and entropy optimization: A solar water pump implementation, J. Mol. Liq. 361 (2022) 119608, https://doi.org/10.1016/j.molliq.2022.119608.
[30]. Santra, A.K., Sen, S., Chakraborty., N: Study of heat transfer due to laminar flow of copper-water nanofluid through two iso-thermally heated parallel plates, Int J Therm Sci., V.48, 391-400(2009).
[31]. Shaiq S., Maraj E.N., Iqbal Z., Remarkable role of C3H8O2 on transportation of MoS2/SiO2 hybrid nanoparticles influenced by thermal deposition and internal heat generation, J. Phys. Chem. Solids. 126 (2019) 294–303.
[32]. Shamshuddin MD., Salawu S.O., Kanayo Kenneth Asogwa, Srinivasa Rao P.: Thermal exploration of convective transportation of ethylene glycol based magnetized nanofluid flow in porous cylindrical annulus utilizing MOS2 and Fe3O4 nanoparticles with inconstant viscosity, Journal of Magnetism and Magnetic Materials 573 (2023) 170663, https://doi.org/10.1016/j.aej.2020.11.019
[33]. Sheikholeslami M, Ganji DD, Javed MY, Ellahi R. Effect of thermal radiation on magnetohydrodynamics nanofluid flow and heat transfer by means of two phase model. J MagnMagn Mater; 374:36–43 (2015).
[34]. Sree Devi, G., Raghavendra Rao, R., Chamka, A.J and Prasada Rao, D.R.V: Mixed convective heat and mass transfer flow of nanofluids in concentric annulus with constant heat flux, Procedia Engineering, 127, 1048-1055(2015).
[35]. Sudarsana Reddy, P., Chamka, A.J: Soret and Dufour effects on MHD convective flow of Al2O3-water and TiO2-water nanofluids past a stretching sheet in porous media with heat generation/absorption, J. Advanced Powder Technology, V. 27, 1207-1218(2016).
[36]. Sulochana G and Ramakrishna G N : Effect of Heat Sources on Non-Darcy Convective Heat and Mass Transfer Flow of Nanofluids in Cylindrical Annulus, *International Journal of Mathematical Archive (IJMA)*, Issue 6, Vol. 8, pp. 53-62 (2017), ISSN 2229-5046.
[37]. Umair Khan, A. Zaib & Fateh Mebarek-Oudina: Mixed Convective Magneto Flow of SiO2–MoS2/C2H6O2 Hybrid Nanoliquids Through a Vertical Stretching/Shrinking Wedge: Stability Analysis, Volume 45, pages 9061–9073, (June 2020)
[38]. Vijayalakshmi,P:Effect of thermal radiation on non-darcy hydromagnetic convective heat and mass transfer flow of water-swcnt's nanofluid in a cylindrical annulus with thermo-diffusion and chemical reaction ,Journal of Xi's University of Archetecture and Technology,Issn No.1006-7930,V.Xiii,Issue.3,pp.16-29(2021)
[39]. Yin,C,L.Zheng,C.Zhang, and X.Zhang:Flow and Heat transfer of Nanofluids over a rotating Disk with uniform stretching rate in the radial direction,Propeller Power Research,V.6,pp.25-30(2017)
[40]. Zhang J, Ahmed A, Naveed Khan M, Wang F, Abdelmohsen, SA and Tariq H. Swirling flow of fluid containing, (SiO2) and (MoS2) nanoparticles analyze via Cattaneo-Christov theory. *J Appl Biomater Funct Mater* 2022; 20: 22808000221094685.
[41]. Zhang Y. *et al.*Solvent-free ionic molybdenum disulphide (MoS_2) nanofluids, J. Mat. Chem. (2012)
[42]. Zhang,C,L.Zheng,X.hang and C.Chen:MHD flow and radiation heat transfer of nanofluids in poprous media with variable surface heat flux and chemical reaction,Applications Mathematical Modern,V.39,pp.165-1821(2015)